

## Complementary Detection of Prostate-Specific Antigen Using In<sub>2</sub>O<sub>3</sub> Nanowires and Carbon Nanotubes

Chao Li,<sup>†</sup> Marco Curreli,<sup>‡</sup> Henry Lin,<sup>§</sup> Bo Lei,<sup>†</sup> F. N. Ishikawa,<sup>†</sup> Ram Datar,<sup>§</sup> Richard J. Cote,<sup>§</sup> Mark E. Thompson,<sup>‡</sup> and Chongwu Zhou<sup>\*†‡</sup>

Departments of Electrical Engineering, Chemistry, and Pathology, University of Southern California, Los Angeles, California 90089

Received June 8, 2005; E-mail: chongwuz@usc.edu

Nanostructured devices, fabricated using single-walled carbon nanotubes<sup>1</sup> (SWNTs), silicon nanowires<sup>2</sup> (Si NWs), or metal oxide nanowires<sup>3</sup> (e.g., In<sub>2</sub>O<sub>3</sub> NWs), are good candidates to manufacture future generations of biosensors. Nanotubes and nanowires have very high surface-to-volume ratios and, therefore, promise very high sensitivities. Recent biosensing literature has reported the use of either carbon nanotubes or nanowires as successful sensors for a number of biological analytes;<sup>1,2</sup> however, combining these two nanomaterials may offer an interesting comparison and also novel sensing strategies. In addition, while several functionalization techniques have been developed to attach antibodies to SWNTs and Si NWs,<sup>1,2</sup> little has been reported for biofunctionalization of metal oxide NWs (e.g., In<sub>2</sub>O<sub>3</sub> and SnO<sub>2</sub>), which are traditionally the key materials for sensing.

In this paper, we report complementary detection of prostate-specific antigen (PSA) using n-type In<sub>2</sub>O<sub>3</sub> nanowires and p-type carbon nanotubes. PSA is an oncological marker for the presence of prostate cancer, which is the most frequently diagnosed cancer among men in the U.S.<sup>4</sup> Despite its utmost importance, detection of PSA using NWs/SWNTs has not been reported. We have made two key innovations. First of all, a novel approach has been developed to covalently attach antibodies to In<sub>2</sub>O<sub>3</sub> NW surfaces via the onsite surface synthesis of a succinimidyl linking molecule. Second, we have combined In<sub>2</sub>O<sub>3</sub> NWs and SWNTs for the detection of PSA, which revealed complementary electrical response upon PSA binding. Furthermore, detection of PSA in solution has been demonstrated to be effective as low as 5 ng/mL, a level useful for clinical diagnosis of prostate cancer.<sup>4</sup>

The device structure of nanowire/nanotube sensors is schematically shown in Figure 1a, where an active channel made up of nanowires or nanotubes bridges the source/drain electrodes, and the silicon substrate can be used as gate.<sup>5</sup> We have used both individual and mat nanowires/nanotubes as the active channel, as described below. Key to selective detection of PSA is to functionalize the nanochannel surface with anti-PSA monoclonal antibody (PSA-AB), a specific ligand for PSA protein. The functionalization strategy adopted for In<sub>2</sub>O<sub>3</sub> NWs is shown in Figure 1b. In<sub>2</sub>O<sub>3</sub> NW devices were first submerged in a solution of 3-phosphonopropionic acid, resulting in binding of the phosphonic acid to the indium oxide surface with the COOH groups available for further reaction. We have previously demonstrated that phosphonic acids strongly bind to indium oxide surfaces and are stable under a variety of conditions.<sup>3a</sup> The COOH groups on the nanowire surface were subsequently converted to a carboxylate succinimidyl ester via incubation in *N,N'*-dicyclohexylcarbodiimide (DCC) and *N*-hydroxysuccinimide<sup>5</sup> and treated with a buffered saline solution of

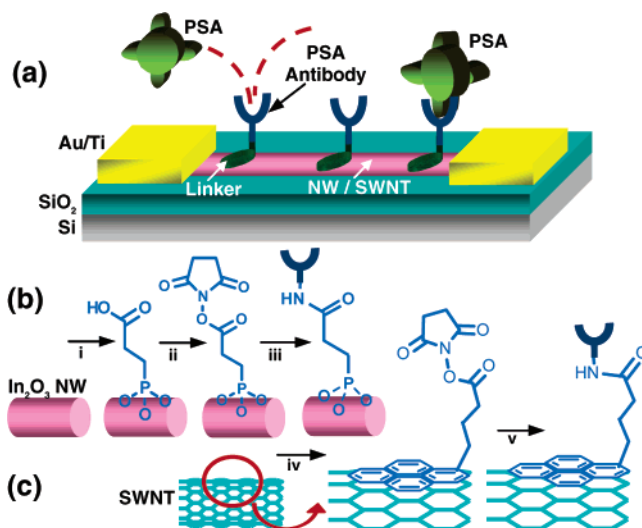


**Figure 1.** (a) Schematic diagram of the nanosensor. PSA-ABs are anchored to the NW/SWNT surface and function as specific recognition groups for PSA binding. (b) Reaction sequence for the modification of In<sub>2</sub>O<sub>3</sub> NW: *i*, deposition of 3-phosphonopropionic acid; *ii*, DCC and *N*-hydroxysuccinimide activation; *iii*, PSA-AB incubation. (c) Reaction sequence for the modification of SWNT: *iv*, deposition of 1-pyrenebutanoic acid succinimidyl ester; *v*, PSA-AB incubation.

PSA-AB at 50  $\mu$ M concentration. The antibody is thus anchored to the nanowire surface. SWNT devices were fabricated by a related procedure, illustrated in Figure 1c. The SWNT surface is first functionalized with 1-pyrenebutanoic acid succinimidyl ester,<sup>1c</sup> followed by treatment with the PSA-AB solution.

Our first step after anchoring PSA-AB to the NW and SWNT devices was to investigate the chemical gating effect of PSA on the devices.<sup>5</sup> We incubated devices consisting of both individual NWs and individual semiconducting SWNTs in a PBS buffered solution containing PSA for  $\sim$ 15 h, at a concentration of 1  $\mu$ g/mL. The device surface was then thoroughly rinsed with deionized water and dried under a stream of nitrogen. The electrical properties of the devices, including both current–voltage ( $I$ – $V_{ds}$ ) and current–gate voltage ( $I$ – $V_g$ ) characteristics, were measured in air before and after the PSA incubation. We consistently observed enhanced conductance for NW devices and reduced conductance for SWNT devices after PSA incubation, as shown in Figure 2a and c, respectively. In addition to the complementary change in conductance, the gate dependence of both the NW and SWNT devices also changed. As shown in Figure 2b and d, the threshold voltage ( $V_T$ ) of the NW device shifted from  $-8$  to  $-14$  V, in contrast to a shift from  $-22$  to  $-25$  V for the SWNT device. This complementary response in conductance can be understood as In<sub>2</sub>O<sub>3</sub> NWs are n-type and SWNTs are p-type semiconductors. The origin of the

<sup>†</sup> Department of Electrical Engineering.

<sup>‡</sup> Department of Chemistry.

<sup>§</sup> Department of Pathology.

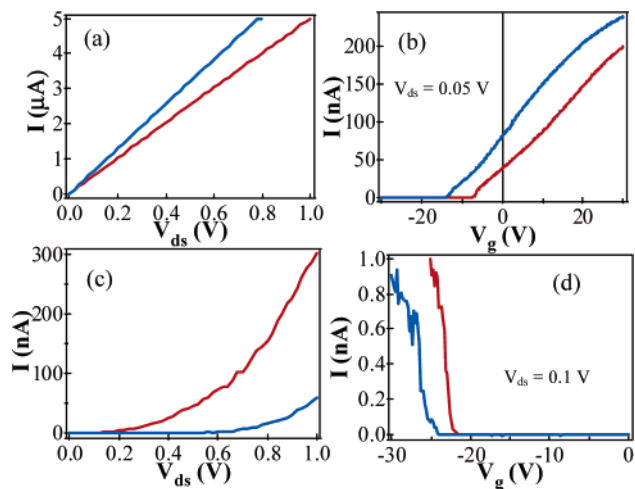


**Figure 2.**  $I$ - $V$  and  $I$ - $V_g$  curves of an  $\text{In}_2\text{O}_3$  nanowire device (a, b) and a SWNT device (c, d) before and after PSA incubation. Red and blue curves represent measurements performed before and after PSA incubation, respectively.

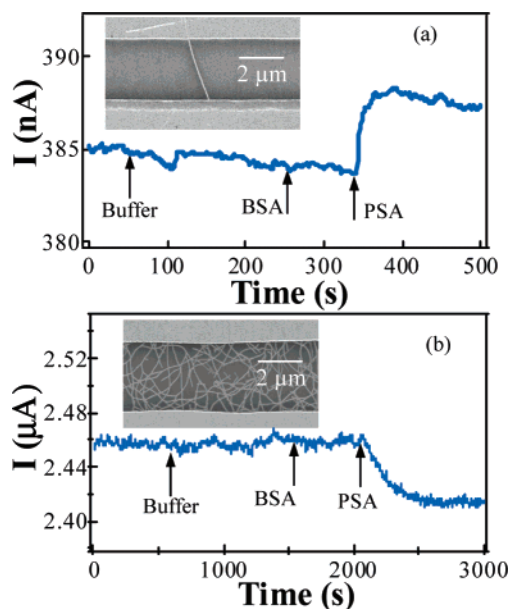


**Figure 3.** Current recorded over time for an individual  $\text{In}_2\text{O}_3$  NW device (a) and a SWNT mat device (b) when sequentially exposed to buffer, BSA, and PSA. Insets: SEM images of respective devices.

change of the device characteristics is that the chemical gating effect of PSA introduces carriers into  $\text{In}_2\text{O}_3$  NWs, leading to enhanced conductance, while the PSA binding decreases the carrier concentration in nanotubes, thus reducing the conductance. Control samples for both kinds of devices went through incubation in buffer without PSA and showed little change in electrical properties before and after the incubation.

We have further performed real-time PSA detection in PBS solution with both  $\text{In}_2\text{O}_3$  NW and SWNT devices. Figure 3 insets display the device images. We used SWNT mat devices in order to overcome the instability found with individual SWNT devices. The antibody-functionalized nanosensors were submerged in PBS buffer solution. The electrical currents through the NW and the SWNTs devices were monitored as several solutions were then added to the solution above the nanosensor. First, additional buffer solution was added to test the nanosensor stability. Next a solution of nontarget bovine serum albumin (BSA) was added, followed by a solution of PSA. The resulting current versus time curves are

shown in Figure 3, (a) for a single  $\text{In}_2\text{O}_3$  NW device ( $V_{ds} = 100$  mV) and (b) for a SWNT mat device ( $V_{ds} = 5$  mV) (time points for each addition are indicated in Figure 3). The current readings from both devices displayed little change after the addition of the buffer solution, thus attesting to the sufficiently high stability of the devices. Upon the addition of 100 nM BSA in PBS, the readings still did not show any appreciable change, indicating nonspecific binding of BSA was successfully suppressed.<sup>6</sup> In sharp contrast, the current of the nanowire device increased rapidly after being exposed to 0.14 nM (5 ng/mL) PSA, while the current of the SWNT mat device decreased relatively slowly and stabilized at lower values upon exposure to 1.4 nM (50 ng/mL) PSA. The amplitude of the current change was about 1.3% for the NW device and 2% for the nanotube devices. We note that the signal-to-noise ratio is about 20 for the NW device exposed to 5 ng/mL PSA (Figure 3a), indicating that the detection limit could approach 250  $\mu\text{g}/\text{mL}$ . Detection of PSA of different concentrations is currently being carried out. Further optimization may lead to nanosensors with sensitivities competitive to those offered by current analytical techniques<sup>7</sup> while providing additional advantages, such as reduced cost, minimal blood sample volume, direct electrical readout, and an ability to perform multiplexed detection for many biomarkers.

In summary, we have demonstrated complementary biosensing using  $\text{In}_2\text{O}_3$  nanowire and SWNT devices for the detection of PSA. Specificity was gained via proper surface functionalization, including a novel approach developed to covalently attach PSA antibodies to  $\text{In}_2\text{O}_3$  NW surfaces. In addition, electronic characterization revealed enhanced conduction for  $\text{In}_2\text{O}_3$  nanowire devices and suppressed conduction for SWNT devices upon PSA exposure, with sensitivity demonstrated down to 5 ng/mL for real-time detection in a buffer at physiological concentration. The combination of n-type NWs and p-type SWNTs shows great promise for the selective detection of desired biomolecules for health care and biomedical research. We believe this work will significantly advance the incorporation of nanomaterials into medically relevant biosensors.

**Acknowledgment.** We acknowledge support from the DARPA MolApps Program (SPAWAR SysCtr San Diego, #N66001-04-1-8902) and the NSF ERC program.

**Supporting Information Available:** Materials, device fabrication, surface functionalization, and control experiments. This material is available free of charge via the Internet at <http://pubs.acs.org>.

## References

- (1) (a) Chen, R. J.; Bangsaruntip, S.; Drouvalakis, K. A.; Shi Kam, N. W.; Shim, M.; Li, Y.; Kim, W.; Utz, P. J.; Dai, H. *Proc. Natl. Acad. Sci. U.S.A.* **2003**, *100*, 4984. (b) Star, A.; Gabriel, J. P.; Bradley, K.; Gruner, G. *Nano Lett.* **2003**, *3*, 459. (c) Chen, R. J.; Zhang, Y.; Wang, D.; Dai, H. *J. Am. Chem. Soc.* **2001**, *123*, 3838. (d) Nguyen, C. V.; Delzeit, L.; Cassell, A. M.; Li, J.; Han, J.; Meyyappan, M. *Nano Lett.* **2002**, *2*, 1079. (e) Koehne, J. E.; Chen, H.; Cassell, A. M.; Ye, Q.; Han, J.; Meyyappan, M.; Li, J. *Clin. Chem.* **2004**, *50*, 1886.
- (2) (a) Patolsky, F.; Lieber, C. M. *Mater. Today* **2005**, *8*, 20. (b) Bunimovich, Y. L.; Ge, G.; Beverly, K. C.; Ries, R. S.; Hood, L.; Heath, J. R. *Langmuir* **2004**, *20*, 10630.
- (3) (a) Curreli, M.; Li, C.; Sun, Y.; Lei, B.; Gundersen, M. A.; Thompson, M. E.; Zhou, C. *J. Am. Chem. Soc.* **2005**, *127*, 6922. (b) Li, C.; Zhang, D.; Han, S.; Liu, X.; Tang, T.; Zhou, C. *Adv. Mater.* **2003**, *15*, 143. (c) Tang, T.; Liu, X.; Li, C.; Lei, B.; Zhang, D.; Rouhanizadeh, M.; Hsiai, T.; Zhou, C. *Appl. Phys. Lett.* **2005**, *86*, 103903. (d) Arnold, M.; Avouris, P.; Pan, W.; Wang, Z. L. *J. Phys. Chem. B* **2003**, *107*, 659.
- (4) (a) Li, X.; Zhang, Y. P.; Kim, H. S.; Bae, K. H.; Stantz, K. M.; Lee, S. J.; Jung, C.; Jimenez, J. A.; Gardner, T. A.; Jeng, M. H.; Kao, C. *Cancer Res.* **2005**, *65*, 1941. (b) Kelloff, G. J.; Coffey, D. S.; Chabner, B. A.; Dicker, A. P.; Guyton, K. Z.; Nisen, P. D.; Soule, H. R.; D'Amico, A. V. *Clin. Cancer Res.* **2004**, *10*, 3927.
- (5) For experimental details, see the Supporting Information.
- (6) Devices with untreated SWNTs show significant BSA binding; see Supporting Information.
- (7) Acevedo, B.; Perera, Y.; Ruiz, M.; Rojas, G.; Benitez, J.; Ayala, M.; Gavilondo, J. *Clin. Chim. Acta* **2002**, *317*, 55.

JA053761G